Proceedings of the 48th National Conference on Fluid Mechanics and Fluid Power (FMFP)
December 27-29, 2021, BITS Pilani, Pilani Campus, RJ, India.

FMFP2021–09–067

Power Harvesting from VIV of Rigidly-coupled Cylinders in Tandem arrangement

Abhijit Pal[1], Atul K. Soti[1]

[1]Department of Mechanical Engineering, IIT Guwahati, Guwahati-781039, India

ABSTRACT

Power harvesting from vortex-induced vibration (VIV) is a fairly new regime that needs to be explored. A practical VIV-based hydroelectric farm will employ a number of devices undergoing VIV. The present work aims to quantify the energy extraction capability of two rigidly-coupled circular cylinders of equal diameter (D) in tandem arrangement. The energy extraction process is modeled using a damper attached to the vibrating cylinders. The cases with different damping ratios (ζ) are numerically simulated by OpenFOAM, an Open-source software computational fluid dynamics solver. The cylinders are rigidly-coupled and oscillate rigidly in the cross-flow direction. All the cases were simulated at a constant mass ratio, defined as the ratio between net oscillating mass to the mass of displaced fluid, 2 and Reynolds number 150. The gap ratio (L/D), defined as the normalized center-to-center distance between the cylinders in flow direction, is taken as 2. The damping ratio is varied in the range of $\zeta = 0.025$–0.10, and the reduced velocity (U^*) is varied from 3 to 8.5. At the smallest damping, the cylinders vibrate with significant amplitude in the reduced velocity range of 4–6, the synchronization region. A maximum vibration amplitude (y/D) value of 0.51 is observed close to reduced velocity 5 at the smallest damping. This value is close to that of an isolated circular cylinder. The vibration amplitude decreases with increasing damping as some of its kinetic energy is dissipated, which is assumed to equal the extracted power in the present case. The width of the synchronization region also decreases with increasing damping. The mean extracted power is maximized at certain reduced velocities in the synchronization region at each damping value. The extracted power is proportional to both damping and vibration amplitude. Since the vibration amplitude reduces with damping, an optimal damping value at which a peak value of the maximum extracted power is obtained. For the present case, the non-dimensional peak extracted power is close to 0.069 at $\zeta = 0.04$ and $U^* \approx 4.5$.

Keywords: Power Harvesting, Vortex-Induced Vibration, Rigidly-coupled Cylinder, Tandem arrangement.

I. INTRODUCTION AND LITERATURE REVIEW

When a flexibly mounted bluff body is placed in a fluid stream, the body experiences unsteady fluid forces. The difference in pressure distribution around the body arises and consequently motion in the body. The non-linear interaction occurs when the motion of the body modifies the flow. This phenomenon is called flow-induced vibration (FIV) or flow-induced motion (FIM). Vortex-induced vibration (VIV) is a resonance type FIV where the frequency of the shed vortices behind the body synchronizes with the body's natural frequency. The shed vortices give rise to unsteady fluid forces that induce motion of the body in the direction normal to the flow.

VIV is considered a destructive phenomenon primarily observed in slender structures like marine risers and long tethered structures in the ocean. But in recent years, a search for clean energy observes another application of VIV, i.e., power extraction capabilities of VIV. Bernitsas et al. [1] were the first to use VIV as a source of clean energy. They made VIVACE (Vortex-induced vibration aquatic clean energy) setup in which the kinetic energy from the body motion can be converted to useful electrical energy. Soti et al. [2] numerically investigated VIV of single-cylinder at Reynolds number (Re) ≤ 200. They have observed there is an optimal damping ratio ζ where the maximum power is obtained. They have also observed that the power strongly depends on Re. The primary reason is maximum amplitude is a strong function of Re. Lee and Bernitsas [3] experimented on VIVACE converter at high Re ($4\times10^4 < \text{Re} < 1.2\times10^5$) where they made a damper-spring apparatus that can virtually change the stiffness and damping. As no energy is harvested at $\zeta = 0$ and very high damping, there is no power due to no oscillation; there is always a ζ (here $\zeta = 0.12$) where the energy is maximum. They have also observed with the increase in stiffness, the maximum extracted power also increases. Sun et al. [4] also got increased power with increased stiffness. In the galloping regime, as the amplitude increases with U^*, the power also increases. Barrero-Gil et al. [5] numerically simulated forced vibration of a single cylinder. They have found maximum efficiency depends upon both ζ and m^*. With increasing $m^*\zeta$, efficiency first increases up to a certain value and then decreases. So, there is an optimal mass-damping parameter $m^*\zeta$ where we get maximum efficiency. They have also pointed out that at low m^*, the spectrum of U^* for significant efficiency is observed, increases.

The extracted power also depends upon the number of cylinders and their relative arrangements. This observation comes from the increase in amplitude with the number of cylinders [6]–[8]. Most of the investigations are carried out for the case of the upstream cylinder being stationary, i.e.,

S. Bhattacharyya and H. Chattopadhyay (eds.), *Fluid Mechanics and Fluid Power (Vol. 1)*,
Lecture Notes in Mechanical Engineering, https://doi.org/10.1007/978-981-19-7055-9_53

wake-induced vibration. Ding et al. [9] performed numerical and experimental investigation on independently moving cylinders in tandem. They have found suppressed VIV for the downstream cylinder at higher Re (Re $> 9.5\times10^4$) in the experiment due to neglecting the free-surface effect in numerical simulation. In their later study, they have simulated the cases of three and four cylinders also. They have got reduced maximum amplitude in the downstream cylinders than the upstream cylinder [10]. Zhao et al. [11] numerically simulated rigidly coupled cylinder in tandem and side-by-side arrangement at low Re = 150. For tandem arrangement, the amplitude is increasing in the upper branch with the normalized center-to-center distance between cylinders in streamwise direction (L/D), and the maximum amplitude shifts to the higher value of U^* with increasing L/D. But surprisingly enough, for side-by-side arrangement apart from T/D = 1.5, the amplitude response curves of other T/D cases hug the single-cylinder case closely. Mechanism of independently moving two-cylinders are different from the rigidly-coupled cylinders as it involves gap flow and VIV [12]. Here T/D represents the center-to-center distance between cylinders in crossflow direction.

The power extracted from the multiple-cylinder arrangement is far higher than the single cylinder. The extracted power also depends upon the distance between the cylinders. Kim and Bernitsas [13] introduced a term 'synergy,' which is the energy extracted from the multiple cylinders divided by the number of cylinders and energy extracted from a single cylinder. Three and four cylinders in tandem can give up to two times more synergy than the single-cylinder, and any cylinder arrangement can give synergy more than one. They have also noticed that at particular U^*, there is some optimal distance for which synergy is highest. But efficiency increases as the number of cylinders and spacing increases. Sun et al. [14] got a steady rise in power in the VIV regime with the increase in L/D. But there is a sharp drop in power for high L/D (L/D = 2.57) in the transition regime due to separation of VIV and galloping.

This study focuses on the power extraction capability of VIV of two cylinders in tandem at L/D = 2.0. The distance is kept at L/D = 2.0 from the practical point of view, as in reality, the cost of making the tandem VIV arrangement will increase, and the power-to-volume ratio will decrease if we increase L/D. Also, the lift coefficient of stationary cylinders in tandem at L/D = 1.5 [12], is smaller than the case for stationary L/D = 2.0 [15]. This reduces the extracted power. As the increasing number of cylinders increases extracted power, VIV of two rigidly-coupled cylinders in tandem is simulated, and extracted power is calculated. The mass ratio is kept at 2, and all the flow is simulated at Re =150. The reduced velocity, U^*, is varied from 3.0 to 8.5, and the damping ratio is varied from ζ = 0.025-0.10. It is hypothesized that using more than one cylinder is beneficial in energy extraction. The cylinders are rigidly-coupled and at a fixed distance of 2D. Is extracted power of two cylinders at tandem at a distance of 2D more than the single-cylinder is answered here.

II. METHODOLOGY

In the present study, the flow simulation is carried out in the open-source CFD tool OpenFOAM, based on C++ libraries and uses an FVM-based solver. For the fluid flow, unsteady incompressible Navier-Stokes (NS) are solved along with the continuity equation. Non-dimensional NS equation is written as:

$$\frac{\partial \mathbf{u}}{\partial t} + (\nabla.\mathbf{u})\mathbf{u} \quad = \quad -\nabla p + \frac{1}{Re}(\nabla^2\mathbf{u}) \tag{1}$$

And continuity equation:

$$\nabla.\mathbf{u} \quad = \quad 0 \tag{2}$$

For the motion of the body, a classical mass-damper-spring oscillator model is used. In the model, the body is constrained to move in the transverse direction with respect to the incoming flow.

$$m\ddot{y} + c\dot{y} + ky = F(t) \tag{3}$$

The above equation can be non-dimensional by non-dimensional parameters as follows:

$$\ddot{Y} + \frac{4\pi\zeta}{U^*}\dot{Y} + \frac{4\pi^2}{U^{*2}}Y = \frac{2}{\pi}\frac{C_L}{m^*} \tag{4}$$

Where, $Y = y/D$ and $C_L = \frac{F_y}{\frac{1}{2}\rho U^2 D}$ are the non-dimensional transverse displacement and lift coefficient respectively. Extracted power is modeled as the power dissipated by the damper, which is $c\dot{y}^2$. So, the non-dimensional instantaneous power can be written as:

$$P(t) = \frac{c\dot{y}^2}{\frac{1}{2}\rho U^3 D} \tag{5}$$

The non-dimensional average power can be written as:

$$\bar{P} = \frac{2\pi^2\alpha}{U^*}U_{rms}^2 \tag{6}$$

Where, α is the mass-damping parameter and U_{rms} is defined as $U_{rms} = \sqrt{\frac{1}{T}\int_0^T \dot{Y}^2 dt}$

The computational domain of $50D\times40D$ is simulated for the two-cylinder case. The schematic of the computational domain is shown in figure 1. The upstream cylinder is 19D from the inlet and 39D from the outlet. The distance of the cylinder center from the wall in the transverse direction is 20D. The center-to-center between cylinder is 2D. Mass ratio, m^* is kept 2 for all the cases of U^*. U^* is varied from 3 to 8.5, and the damping ratio ζ is varied from 0.025 to 0.1. Initially the fluid is moving with a constant uniform velocity U=1. In inlet, the pressure boundary condition is zero gradient. The outlet boundary condition is zero gradient ($\frac{\partial u}{\partial x} = 0$ and $\frac{\partial v}{\partial x} = 0$). As it is a 2D simulation, front and back boundary conditions are empty, i.e., no computation is done on those faces. The top and bottom faces are symmetry ($\frac{\partial u}{\partial y} = 0$ and $v = 0$).

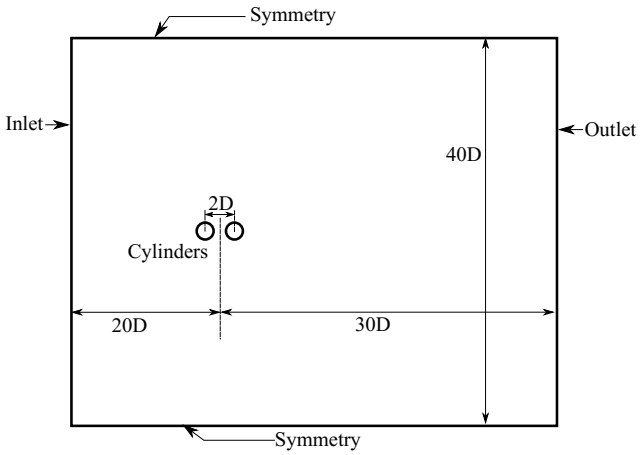

Figure 1: **Schematic of Computational Domain**

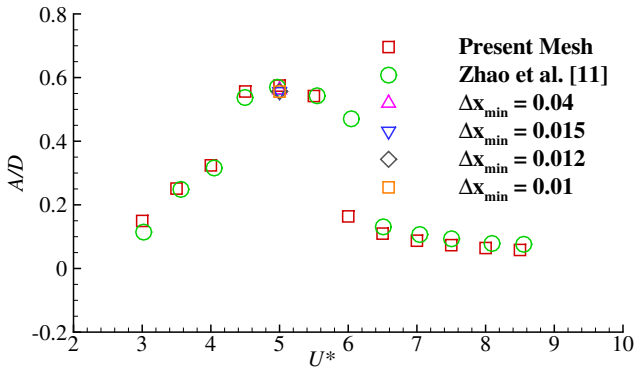

Figure 2: **Numerical validation of amplitude data with Zhao et al. [11] at L/D = 2.0, ζ = 0 and Mesh independency test**

A. **Validation**

Mesh independency test has been shown in the figure 2. Minimum mesh size Δx_{min} is varied 0.04, 0.02, 0.015, 0.012 and 0.01. The amplitude data at U^* = 5.0 and ζ = 0 is taken as test data. Range of number of cells for the varied Δx_{min} are 11139, 22197, 37440, 54590 and 77058 respectively. The deviations of amplitude data for other meshes are within 1%.The numerical setup is validated with Zhao et al. [11] of tandem ctlinder at L/D = 2.0 and ζ = 0. The validation results are also shown in figure 1. The amplitude response is in good agreement with our results except at U^* = 6.0. The reason could be due to the hysteric nature of VIV [16].

III. RESULTS AND DISCUSSION

A. **Amplitude Response**

Figure 3 shows the transient vibration response curve at different U^*. It has been observed that at low U^* = 3.00, the amplitude grows and becomes stable at around timestep 500. But in U^* = 4.00, the amplitude stabilizes at earlier timestep. We get highest amplitude of 0.51D at U^* = 5.00 at ζ = 0.025. We have also observed that at ζ = 0.025, with the increase in U^*, the beating phenomenon is prevalent. With increasing ζ, the amplitude slowly diminishes and becomes more stable. The beating phenomenon is not observed at higher ζ. With the increase in U^*, the period of beating increases. Due to beating, the amplitude increases slowly and then decreases. At any particular U^* also with increasing ζ the amplitude decreases, and the time period of beating increases.

Figure 4 shows the variation of amplitude at different ζ with varying U^*. No upper branch is visible at low Re; only initial and lower branches are present in the vibration response. It is observed that with the increase in ζ, the maximum amplitude decreases, and the synchronization regime gets narrower. In the initial branch of amplitude response, the amplitude decreases with the increase in ζ. The transition from the initial to the lower branch is smooth for all the ζ, i.e., there is no jump. At higher U^*, i.e., $U^* > 6$, the body goes out of synchronization, and the amplitude reduces to a low value. The desynchronization regime starts at an early value of U^* with the increase in ζ. A significant amplitude is observed in the U^* range of 4–6.

B. **Frequency Response**

The variation of frequency response with U^* is plotted in figure 5. The f/f_n is the normalized frequency response. As seen in figure 5 in the initial branch, the frequency is low. For ζ = 0.04, 0.05 and 0.06, there is sharp jump at around U^* = 3.5. The jump is a little bit smeared out for ζ = 0.075 and 0.10. The reason is that at a higher value of ζ, the jump in amplitude response is less, i.e., the amplitude increases gradually. Compared to the single-cylinder, the frequency response initiates at a rather high value. The frequency response is increasing with increasing U^*, but it does not overlap with the shedding frequency of the non-oscillatory body or the St = 0.2 line. There is no jump in the lower branch, as seen in figure 5 and there is a smooth transition between the initial and the lower branches.

C. **Phase Difference**

Phase difference (ϕ) is calculated from the difference in phase between lift force and displacement, and it is plotted in the figure 6. There is a jump in phase observed near U^* = 5.5–6 at lower values of ζ. With the increase in ζ, the jump in phase is gradual. So, at low ζ values, ϕ remains 0°, where at higher ζ change in ϕ starts earlier. This jump-in phase is associated with the cylinders going into desynchronization. From figure 5 we can see that when normalized frequency f/f_n is less than 1, the phase difference is 0° and when it is greater than 1 the phase difference jumps to 180°. The jump from 0° to 180° happens when f/f_n crosses 1 at U^* = 6. In the higher values of ζ, this process starts early. A sharp jump in phase difference is observed at lower ζ. For ζ = 0.06, 0.075, and 0.10, the phase difference gradually changes from 0 to a higher value. For ζ = 0.10, at around U^* = 5.5 the value of ϕ reaches up to 90°.

D. **Flow Patterns**

The vorticity contours at U^* = 4.5 and U^* = 5.0, ζ = 0.025 are plotted in the figure 7. It is observed that the cylinder changes direction from the mean position from t/T = 111.1 to 120. In the figure 7(a), the cylinders are

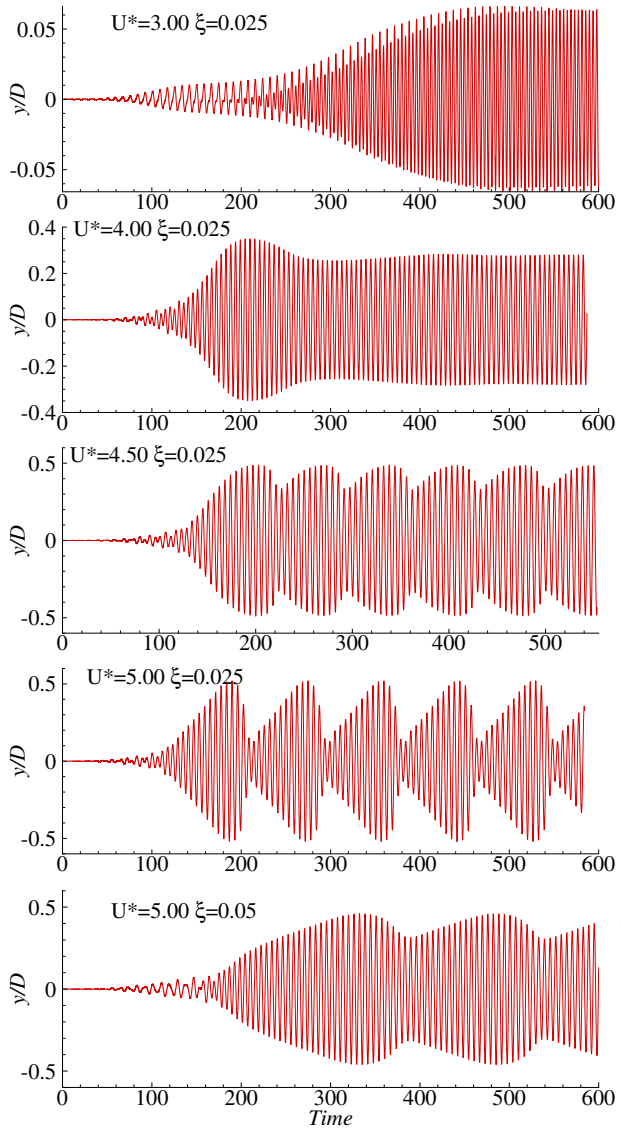

Figure 3: **Transient amplitude response at different** U^* **and** ζ

moving up, and in figure (b), the cylinders are moving downwards. The vortices from the upstream cylinder detach from the surface and impinge on the downstream cylinder. The vortices roll up to the leading edge of the downstream cylinder. In figure 7(b), the lift force of the downstream cylinder becomes very small because the clockwise vortices shed from the upstream cylinder cancel out the counter-clockwise vortices from the downstream cylinder. 2S type of vortices shed from each cycle of vibration, i.e., two single vortices shed in a single cycle like von-kàrman vortex-street. We can also see that as the cylinder changes the direction of displacement, the width of the vortex street increases.

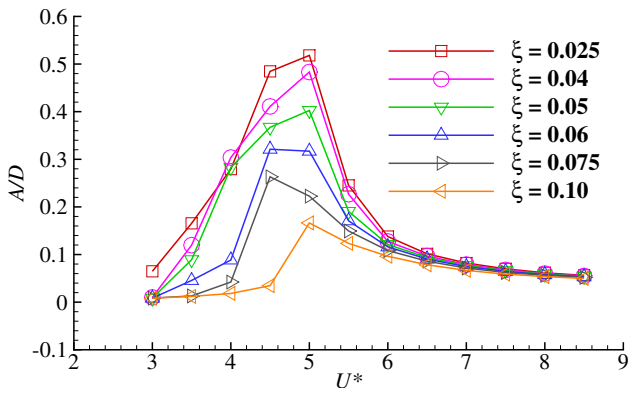

Figure 4: **Variation of amplitude response with** U^* **at particular damping ratios**

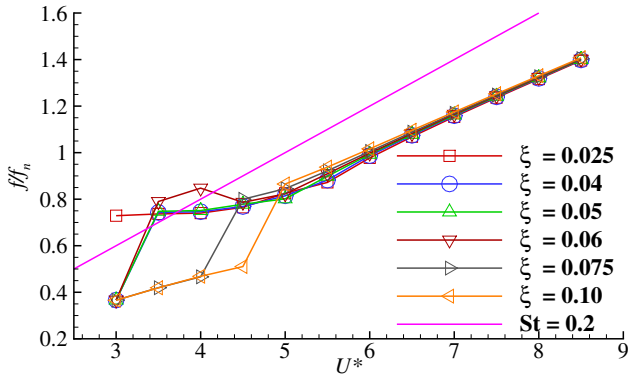

Figure 5: **Frequency response at different** ζ **with the variation of** U^*

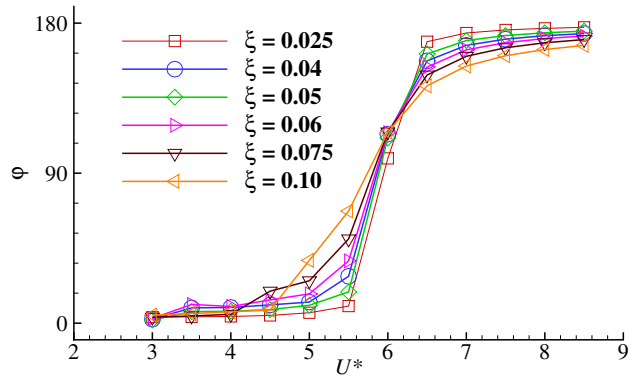

Figure 6: **Variation of phase difference at different** ζ

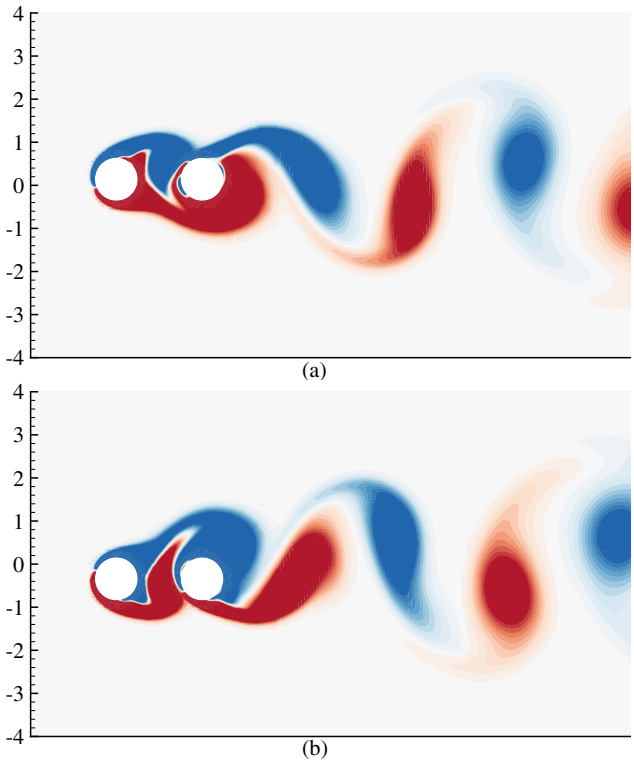

Figure 7: Vorticity contour at timestep t/T = (a) 111.1 and (b) 120 at U^* = 5.0 and ζ = 0.025

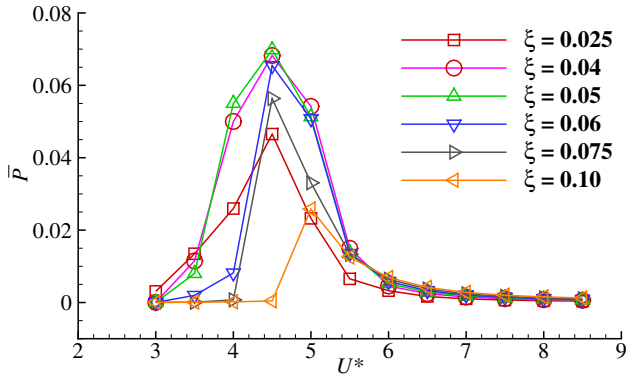

Figure 8: Power extraction at different ζ. Maximum power obtained is 0.069 at U^* = 5.0

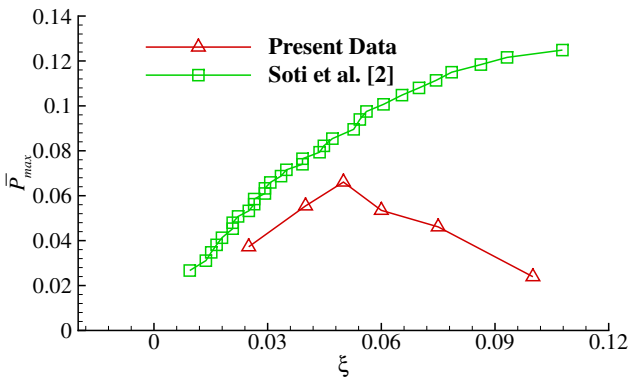

Figure 9: Variation of power extraction with ζ. Comparison of power extraction of tandem cylinders with single cylinder value of Soti et al. [2]. Maximum power obtained for single cylinder is 0.131

E. Power Extraction

The fluctuating lift force generated from the shedding of vortices behind the body is responsible for the oscillations of the flexibly mounted rigid body. The vibration of the cylinders is a means to extract energy from the VIV. From equation 6 it is clear that power is dependent upon m^*, ζ and U^*. In the present work, m^* is constant and taken as 2. Variation of power with ζ and U^* is plotted in the figure 8. It has been noticed that for a particular ζ with the increase in U^*, the power increases to a maximum value and then decreases. This variation of power with U^* corresponds to the fact that amplitude depends upon U^*. With the variation of U^*, we get different regimes of amplitude response. The power variation is similar to that of the amplitude response. But notice that we do not get maximum power at maximum amplitude. We can see that transient power depends on the square of the instantaneous velocity, so the effect of velocity is more than the amplitude itself. We can associate the jump in power with the jump in phase difference also. When the lift force is in phase with the displacement, the power is higher, and power decreases when it is out of phase. The sudden fall in power at U^* = 5.5 for ζ = 0.10 is associated with the change in phase difference ϕ. The fall in power shifts to the left as ζ decreases. From the figure 8, it has been noted that we get maximum power for a particular ζ, and there is always an optimum ζ for which we get maximum optimum power.

In the figure 9, the maximum power at each ζ value is plotted. We see that there is an optimum ζ for which we get the maximum power. For the tandem cylinder case, the maximum non-dimensional power we get is 0.069 at ζ = 0.04, U^* = 4.5. We can also see that at the lower values of ζ, the power is less, and at high values of ζ, the power is small. The reason is power depends upon ζ, so if we decrease ζ to a smaller value, we will get negligible power. Also, the displacement is minimal at a higher value of ζ, so there is no noticeable appreciable power. So there must be some ζ for which the power is maximum. We compare the result of extracted power with that of the single-cylinder from Soti et al. [2]. We see that at ζ = 0.10, the value of non-dimensional power is almost 0.125, double the value of maximum power we get for tandem cylinders. So, we can say that rigidly-coupled two cylinders in tandem at a distance of L/D = 2.0 are not a feasible arrangement of power extraction.

IV. CONCLUSIONS

This paper discussed vortex-induced vibration (VIV) attributes of tandem cylinders at L/D = 2.0. The amplitude response, frequency response, and phase differences are

discussed for the tandem arrangement. Then the power extraction from the cylinders is presented. The highest amplitude is reported 0.51D, which is less than the amplitude value of the single cylinder. Two regimes of amplitude have been observed similar to a single-cylinder at low Re. The amplitude decreases with increasing damping ratio ζ. The higher ζ value follows the transition from upper to lower branch more smoothly. The phase difference is smeared out more as we increase ζ.

The power also shows the same trend as the amplitude. The maximum non-dimensional power is 0.069, and it is observed at U^* = 4.5, ζ = 0.04. With the increase in ζ extracted power decreases. Also, there is an optimum ζ for which the power is maximum. In this case, the optimum ζ is 0.04. But the extracted power from the single-cylinder is almost two times the extracted power from the tandem arrangement. The reason may be the downstream cylinder is greatly affected by the upstream cylinder. The vortices from the upstream cylinder are detached from the surface and roll up to the surface of the downstream cylinder. As the two cylinders acted as the same body and the distance between them is significantly less, the vortices from the upstream cylinder do not have the space to develop and suppress the vortices from the downstream cylinder.

V. ACKNOWLEDGEMENT

The authors would like to acknowledge the financial support from Grant No. SRG/2020/001082, provided by Science & Engineering Research Board (SERB), India. We are also grateful to the Param-Ishan HPC facility at IIT Guwahati for providing the required CPU hours to carry out the necessary computations.

NOMENCLATURE

U	Free stream Velocity	
u	Fluid velocity	
D	Diameter of cylinder	
L	Center-to-center distance between the cylinders in cross-flow direction	
U^*	Reduced velocity	$[\frac{U}{f_n D}]$
Re	Reynolds number	
f_n	Natural frequency of body in water	
ζ	Damping ratio	$[\frac{c}{c_c}]$
m^*	Mass ratio	$[\frac{m}{m_d}]$
m_d	Mass of displaced fluid	
c	Damping constant	
k	Spring constant	
C_L	Lift coefficient	
T	Time period of oscillation	

REFERENCES

[1] M. M. Bernitsas, K. Raghavan, Y. Ben-Simon, and E. Garcia, "Vivace (vortex induced vibration aquatic clean energy): A new concept in generation of clean and renewable energy from fluid flow," 2008.

[2] A. K. Soti, M. C. Thompson, J. Sheridan, and R. Bhardwaj, "Harnessing electrical power from vortex-induced vibration of a circular cylinder," *Journal of Fluids and Structures*, vol. 70, pp. 360–373, 2017.

[3] J. Lee and M. Bernitsas, "High-damping, high-reynolds viv tests for energy harnessing using the vivace converter," *Ocean engineering*, vol. 38, no. 16, pp. 1697–1712, 2011.

[4] H. Sun, E. S. Kim, G. Nowakowski, E. Mauer, and M. M. Bernitsas, "Effect of mass-ratio, damping, and stiffness on optimal hydrokinetic energy conversion of a single, rough cylinder in flow induced motions," *Renewable Energy*, vol. 99, pp. 936–959, 2016.

[5] A. Barrero-Gil, S. Pindado, and S. Avila, "Extracting energy from vortex-induced vibrations: a parametric study," *Applied mathematical modelling*, vol. 36, no. 7, pp. 3153–3160, 2012.

[6] G. d. S. Assi, J. Meneghini, J. Aranha, P. Bearman, and E. Casaprima, "Experimental investigation of flow-induced vibration interference between two circular cylinders," *Journal of fluids and structures*, vol. 22, no. 6-7, pp. 819–827, 2006.

[7] D. Sumner, "Two circular cylinders in cross-flow: a review," *Journal of fluids and structures*, vol. 26, no. 6, pp. 849–899, 2010.

[8] M. Zdravkovich, "Review of interference-induced oscillations in flow past two parallel circular cylinders in various arrangements," *Journal of Wind Engineering and Industrial Aerodynamics*, vol. 28, no. 1-3, pp. 183–199, 1988.

[9] L. Ding, M. M. Bernitsas, and E. S. Kim, "2-d urans vs. experiments of flow induced motions of two circular cylinders in tandem with passive turbulence control for 30,000 $<$ Re $<$ 105,000," *Ocean Engineering*, vol. 72, pp. 429–440, 2013.

[10] L. Ding, L. Zhang, E. S. Kim, and M. M. Bernitsas, "Urans vs. experiments of flow induced motions of multiple circular cylinders with passive turbulence control," *Journal of Fluids and Structures*, vol. 54, pp. 612–628, 2015.

[11] M. Zhao, "Flow induced vibration of two rigidly coupled circular cylinders in tandem and side-by-side arrangements at a low reynolds number of 150," *Physics of Fluids*, vol. 25, no. 12, p. 123601, 2013.

[12] I. Borazjani and F. Sotiropoulos, "Vortex-induced vibrations of two cylinders in tandem arrangement in the proximity–wake interference region," *Journal of fluid mechanics*, vol. 621, pp. 321–364, 2009.

[13] E. S. Kim and M. M. Bernitsas, "Performance prediction of horizontal hydrokinetic energy converter using multiple-cylinder synergy in flow induced motion," *Applied energy*, vol. 170, pp. 92–100, 2016.

[14] H. Sun, C. Ma, E. S. Kim, G. Nowakowski, E. Mauer, and M. M. Bernitsas, "Hydrokinetic energy conversion by two rough tandem-cylinders in flow induced motions: Effect of spacing and stiffness," *Renewable Energy*, vol. 107, pp. 61–80, 2017.

[15] J. Meneghini, F. Saltara, C. Siqueira, and J. Ferrari Jr, "Numerical simulation of flow interference between two circular cylinders in tandem and side-by-side arrangements," *Journal of fluids and structures*, vol. 15, no. 2, pp. 327–350, 2001.

[16] T. Prasanth and S. Mittal, "Vortex-induced vibrations of a circular cylinder at low reynolds numbers," *Journal of Fluid Mechanics*, vol. 594, pp. 463–491, 2008.